



**HAL**  
open science

## Sensitivity analysis for parameter identification in quasi-static poroelasticity

Brice Lecampion, Andrei Constantinescu

► **To cite this version:**

Brice Lecampion, Andrei Constantinescu. Sensitivity analysis for parameter identification in quasi-static poroelasticity. *International Journal for Numerical and Analytical Methods in Geomechanics*, 2005, 29 (2), pp.163-185. 10.1002/nag.409 . hal-00111439

**HAL Id: hal-00111439**

**<https://hal.science/hal-00111439v1>**

Submitted on 15 Feb 2023

**HAL** is a multi-disciplinary open access archive for the deposit and dissemination of scientific research documents, whether they are published or not. The documents may come from teaching and research institutions in France or abroad, or from public or private research centers.

L'archive ouverte pluridisciplinaire **HAL**, est destinée au dépôt et à la diffusion de documents scientifiques de niveau recherche, publiés ou non, émanant des établissements d'enseignement et de recherche français ou étrangers, des laboratoires publics ou privés.



Distributed under a Creative Commons Attribution - NonCommercial 4.0 International License

# Sensitivity analysis for parameter identification in quasi-static poroelasticity

Brice Lecampion<sup>1</sup> and Andrei Constantinescu<sup>2,\*</sup>,<sup>†</sup>

<sup>1</sup>CSIRO Petroleum, Melbourne Office, Bag 10, Clayton South, Vic 3169, Australia

<sup>2</sup>Laboratoire de Mécanique des Solides, CNRS UMR7649, Ecole Polytechnique, 91128 Palaiseau Cedex, France

This paper is devoted to the formulation of the direct differentiation method and adjoint state method in quasi-static linear poroelasticity. We derive the strong and weak formulation of both methods and discuss their solutions using the finite element method. The techniques are illustrated and tested on two numerical examples for the case of isotropic and homogeneous material. The presented formulations can be extended to more complex behaviour in poromechanics.

KEY WORDS: poroelasticity; parameter identification; sensitivity analysis; adjoint state method; direct differentiation method; inverse problems

## INTRODUCTION

Studies of poroelastic materials are encountered in several fields ranging from petroleum geomechanics [1, 2] to biomechanics [3]. In all these problems, there is a need for parameter identification from measured responses to known solicitations.

The complexity of the poroelastic system of equations is such that *only* a small number of closed form solutions is available in the literature. Parameter identification based on closed-form solutions have been presented for some laboratory experiments [4] and *in situ* tests [5]. As a consequence, in most cases, one has to rely on a numerical approximate solution of the particular configuration which has to be coupled with a parameter identification algorithm. This parameter identification process is based in many cases on the minimization of a cost functional measuring the mismatch between simulations and measurements. In order to speed up the minimization, one generally uses gradient algorithms. Gradient-based algorithms, are constructed to converge rapidly to the nearest local minimum. However, let us recall a series of algorithms like simulated annealing, simplex method, genetic algorithms, etc. which are far slower than gradient methods, but might also detect other local minima when the cost functional

---

\*Correspondence to: A. Constantinescu, Laboratoire de Mécanique des Solides, CNRS UMR7649, Ecole Polytechnique, 91128 Palaiseau Cedex, France.

<sup>†</sup>E-mail: andrei.constantinescu@lms.polytechnique.fr

Contract/grant sponsor: French Agency for Radioactive Waste Management (ANDRA)

happens to be non-convex. In the examples discussed next, we only consider the use of gradient-based method for the solution of parameter identification problems and shall present some methods to compute the gradient.

A straightforward way of computing the gradient is the finite difference technique which is easy to apply but presents a series of drawbacks: large computational cost and uncontrolled accuracy. The accuracy depends, on the one hand, on the precision of the numerical simulation and, on the other hand on the parameter step chosen to compute the gradient, which cannot be estimated in advance.

The purpose of this work is to extend the direct differentiation method (DDM) and the adjoint state method (ASM) to the linear quasi-static poroelastic problem. Without entering into much details, we can state that the DDM computes the complete local fields of sensitivities: partial derivative of the poromechanical fields with respect to the parameters to be identified. The ASM computes directly the gradient of a cost functional with respect to the parameters using Lagrangian techniques. Both methods require the solution of auxiliary problems. A general presentation of these techniques can be found in References [6, 7].

These two methods (DDM and ASM) have recently been applied to a series of mechanical problems closely related to poroelasticity. The DDM for semi-coupled poro-plastic materials has been presented in Reference [8] and applied to a synthetic parameter identification problem. For thermal problems, both methods have been discussed in Reference [9], while the ASM has been presented in Reference [10] for the case of thermo-elasticity.

In this paper, we shall derive the strong and weak formulation of both methods in poroelasticity and discuss their solutions using the finite element method. For a general presentation of a solution based on finite element in space and finite difference in time see References [1, 11] and references therein. However, the presented formulations can also be used in relation to the numerical solution of poroelastic problems by other techniques, for example boundary elements [12, 13], displacement discontinuity method [14] for fracture problems, etc.

The paper starts by recalling the strong and weak form of the forward problem. Then, a general formulation of parameter identification problem is given. The next two sections are devoted to the formulation of the DDM and ASM as well as their numerical programming. Finally, the methods are illustrated and tested on two numerical examples.

## THE FORWARD POROELASTIC PROBLEM $\mathcal{P}$

We shall recall in this section the classical forward problem of quasi-static poroelasticity as described by Biot [15, 16], Detournay and Cheng [1] and Coussy [11]. We restrict the presentation to the case of small strain, small displacements and small fluid flow vector. Moreover, for the sake of clarity, we shall consider that the pores are saturated and that the pore fluid is incompressible. The mass conservation therefore reduces to volume conservation (see Reference [11] for the general case and its implications). These hypothesis leads to the classical form of the initial and boundary value problem in poroelasticity [15]. We shall present the strong and weak form of the problem and recall the main lines of its numerical solution using the finite element method.

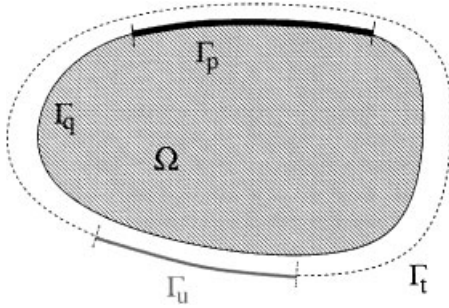


Figure 1. Porous domain  $\Omega$  and the two distinct partition of its boundary  $\Gamma$ .

*Strong formulation of the forward problem*

The porous medium  $\Omega$  of boundary  $\Gamma$  (see Figure 1) is described by two stress-like quantities: its stress state  $\boldsymbol{\sigma}$ , pore pressure field  $p$ , and two strain-like quantities, the solid strain tensor  $\boldsymbol{\varepsilon}$  and the fluid volume content  $\zeta$ . These strain quantities are related to kinematic variables, respectively, the solid displacement vector  $\mathbf{u}$  and the fluid flow vector  $\mathbf{q}$ . We consider that during the time interval  $T = [0, t_f]$ , a quasi-static hydro-mechanical loading is applied on the boundary  $\Gamma$ . The governing equations of the problem can be expressed as follows.

The balance equation is

$$\operatorname{div} \boldsymbol{\sigma} + \mathbf{F} = \mathbf{0} \quad \text{in } \Omega \times T \quad (1)$$

where  $\mathbf{F}$  denotes the total volumetric force.

The compatibility relation between displacements and strains under the assumption of small strains is defined as

$$\boldsymbol{\varepsilon}(\mathbf{u}) = \frac{1}{2}(\nabla \mathbf{u} + \nabla^T \mathbf{u}) \quad \text{in } \Omega \times T \quad (2)$$

The fluid volume balance is given by

$$\dot{\zeta} + g = -\operatorname{div} \mathbf{q} \quad \text{in } \Omega \times T \quad (3)$$

where the time derivatives are denoted by a dot and  $g$  is the fluid source.

Equations (1)–(3) are universal, i.e. they do not depend on the intrinsic behaviour of the porous material. In order to complete the formulation of the linear poroelastic problem, one needs a constitutive relation relating the stress to the strain as well as a transport law relating the fluid flow vector to the pore pressure. In linear poroelasticity, this last relation is given by Darcy's law

$$\mathbf{q} = -\mathbf{k} \cdot (\nabla p - \mathbf{f}) \quad \text{in } \Omega \times T \quad (4)$$

where  $\mathbf{f}$  is the fluid volumetric force,  $\mathbf{k}$  is the hydraulic tensor  $[M^{-1}L^3T]^\ddagger$ , related to the intrinsic permeability  $\boldsymbol{\kappa} [L^2]$  as follows  $\mathbf{k} = \boldsymbol{\kappa}/\mu_f$ , where  $\mu_f$  is the dynamic fluid viscosity  $[ML^{-1}T^{-1}]$ .

<sup>‡</sup>Between brackets, we recall the dimensions of the coefficient.

The linear poroelastic constitutive law can be written in different forms. Here, we choose to express the stress quantities  $(\boldsymbol{\sigma}, p)$  as function of the strain ones  $(\boldsymbol{\varepsilon}, \zeta)$

$$\begin{aligned}\boldsymbol{\sigma} &= (\mathbf{C} + \mathbf{b} \otimes \mathbf{b}M) : \boldsymbol{\varepsilon}(\mathbf{u}) - M\mathbf{b}\zeta \\ p &= M(\zeta - \mathbf{b} : \boldsymbol{\varepsilon}(\mathbf{u}))\end{aligned}\tag{5}$$

where  $\mathbf{C}$  is the tensor of drained elastic moduli  $[ML^{-1}T^{-2}]$ ,  $\mathbf{b}$  is the tensor of Biot coefficients  $[-]$  and  $M$  the Biot's modulus  $[ML^{-1}T^{-2}]$ . We will also use the tensor of undrained elastic moduli  $\mathbf{C}_u = \mathbf{C} + \mathbf{b} \otimes \mathbf{b}M$ .

*Boundary conditions:* Four types of different boundary conditions can be applied on  $\Gamma$ : forces and fluid fluxes corresponding to Neumann type boundary conditions, displacement and pore pressure corresponding to Dirichlet boundaries conditions.

$$\begin{aligned}\boldsymbol{\sigma} \cdot \mathbf{n} &= \mathbf{t}_g \quad \text{on } \Gamma_t \times T \\ \mathbf{q} \cdot \mathbf{n} &= q_g \quad \text{on } \Gamma_q \times T\end{aligned}\tag{6}$$

$$\begin{aligned}\mathbf{u} &= \mathbf{u}_g \quad \text{on } \Gamma_u \times T \\ p &= p_g \quad \text{on } \Gamma_p \times T\end{aligned}\tag{7}$$

We have introduced several subsets of the boundary  $\Gamma$  of the porous medium on which the different boundary conditions are applied during the interval of interest. It is known (see References [1, 11]) that the forward problem is well posed *if and only if* the subsets  $\Gamma_u$  and  $\Gamma_t$ , respectively,  $\Gamma_q$  and  $\Gamma_p$  form two distinct partitions of  $\Gamma$  at each time  $t$  (Figure 1)

$$\begin{aligned}\Gamma &= \Gamma_t \cup \Gamma_u, \quad \Gamma_t \cap \Gamma_u = \emptyset \\ \Gamma &= \Gamma_p \cup \Gamma_q, \quad \Gamma_p \cap \Gamma_q = \emptyset\end{aligned}$$

Also, note, that in the case where only Neumann boundary conditions are applied to the porous solid, the solution of the forward problem is defined up to a rigid body displacement and constant pore pressure field.

*Initial conditions:* The description of the problem would not be complete without the initial conditions. The initial state can be described by an initial stress  $\boldsymbol{\sigma}_0$  and pore pressure  $p_0$  fields. These fields should satisfy the balance equation and fluid continuity equations

$$\begin{aligned}\operatorname{div} \boldsymbol{\sigma}_0 + \mathbf{F}_0 &= \mathbf{0} \quad \text{in } \Omega \\ \boldsymbol{\sigma}_0 \cdot \mathbf{n} &= \mathbf{t}_g(0) \quad \text{on } \Gamma_t\end{aligned}\tag{8}$$

for the initial stress field, and

$$\begin{aligned}\operatorname{div} \mathbf{k} \cdot (\nabla p_0 - \mathbf{f}_0) &= 0 \quad \text{in } \Omega \\ \mathbf{q}_0 \cdot \mathbf{n} &= -(\mathbf{k} \cdot (\nabla p_0 - \mathbf{f}_0)) \cdot \mathbf{n} = q_g(0) \quad \text{on } \Gamma_q \\ p_0 &= p_g(0) \quad \text{on } \Gamma_p\end{aligned}\tag{9}$$

for the initial pore pressure field.

Such an initial poroelastic state can be taken as a reference such that the variables of the linear poroelastic problem can be defined as the variation from this initial state.

*Weak formulation of the problem*

Taking the time derivatives of the balance equation (1), the use of the divergence theorem enables to write the following equation for any vector  $\mathbf{v} \in H^1(\Omega)$  during the time interval  $T$ :

$$\int_{\Omega} \boldsymbol{\varepsilon}(\mathbf{v}) : \dot{\boldsymbol{\sigma}} \, dx = \int_{\Gamma} \mathbf{v} \cdot (\dot{\boldsymbol{\sigma}} \cdot \mathbf{n}) \, dx + \int_{\Omega} \mathbf{v} \cdot \dot{\mathbf{F}} \, dx \quad (10)$$

In a similar manner, from the fluid volume balance equation (3) one obtains for any scalar field  $r \in H^1(\Omega)$  during  $T$

$$\int_{\Omega} \nabla r \cdot \mathbf{q} \, dx - \int_{\Omega} r \dot{\zeta} \, dx = \int_{\Gamma} r \mathbf{q} \cdot \mathbf{n} \, dx + \int_{\Omega} r g \, dx \quad (11)$$

The weak form of the poroelastic problem is obtained by adding the last two equations: (10) + (11). Then, the constitutive (5) and transport laws (4) allow to express this weak form as function of one set of variables, for example  $(\mathbf{u}, p)$  or  $(\boldsymbol{\sigma}, \zeta)$ . In the following, we use the expression of the weak form of the problem using the variables  $(\mathbf{u}, p)$ . This is the classical choice made towards the numerical solution by the finite element method.

For sake of clarity, let us introduce the following bi-linear operators:

- *The elasticity operator:*

$$\mathcal{E}(\mathbf{u}, \mathbf{v}) = \int_{\Omega} \boldsymbol{\varepsilon}(\mathbf{u}) : \mathbf{C} : \boldsymbol{\varepsilon}(\mathbf{v}) \, dx \quad (12)$$

- *The storage operator:*

$$\mathcal{S}(p, r) = \int_{\Omega} p \frac{1}{M} r \, dx \quad (13)$$

- *The diffusivity operator:*

$$\mathcal{A}(p, r) = \int_{\Omega} \nabla p : \mathbf{k} : \nabla r \, dx \quad (14)$$

- *The coupling operator:*

$$\mathcal{C}(p, \mathbf{u}) = \int_{\Omega} p \mathbf{b} : \boldsymbol{\varepsilon}(\mathbf{u}) \, dx = \int_{\Omega} \boldsymbol{\varepsilon}(\mathbf{u}) : \mathbf{b} p \, dx \quad (15)$$

We can see that due to material symmetry together with the symmetry of the small strain and stress tensors, *all* the previously defined bi-linear operators are symmetric, i.e.  $\cdot(a, b) = \cdot(b, a)$ .

The weak form of the quasi-static poroelastic problem can now be expressed as

Find  $\mathbf{u} \in \mathbf{U}$  and  $p \in \mathbf{P}$  such that at all time  $t \in T$ :

$$\begin{aligned} & \mathcal{E}(\dot{\mathbf{u}}, \mathbf{v}) - \mathcal{C}(\dot{p}, \mathbf{v}) - \mathcal{C}(r, \dot{\mathbf{u}}) - \mathcal{S}(\dot{p}, r) - \mathcal{A}(p - p_0, r) \\ & = \int_{\Gamma_t} \mathbf{v} \cdot \dot{\mathbf{t}}_g \, dx + \int_{\Gamma_q} r \mathbf{q}_g \cdot \mathbf{n} \, dx + \int_{\Omega} (\mathbf{v} \cdot \dot{\mathbf{F}} + r g) \, dx \end{aligned} \quad (16)$$

for any tests fields  $\mathbf{v} \in \mathbf{U}_0$  and  $r \in \mathbf{P}_0$ .

where we have defined the functional spaces for the following Dirichlet boundary conditions:

$$\begin{aligned}
\mathbf{U} &= \{\mathbf{u} \in H^1(\Omega) \mid \mathbf{u} = 0 \text{ in } \Omega \text{ at } t = 0; \mathbf{u} = \mathbf{u}_g \text{ on } \Gamma_u \times T\} \\
\mathbf{P} &= \{p \in H^1(\Omega) \mid p = p_0 \text{ in } \Omega \text{ at } t = 0; p = p_g \text{ on } \Gamma_p \times T\} \\
\mathbf{U}_0 &= \{\mathbf{v} \in H^1(\Omega) \mid \mathbf{v} = 0 \text{ in } \Omega \text{ at } t = 0; \mathbf{v} = 0 \text{ on } \Gamma_u \times T\} \\
\mathbf{P}_0 &= \{r \in H^1(\Omega) \mid r = 0 \text{ in } \Omega \text{ at } t = 0; r = 0 \text{ on } \Gamma_p \times T\}
\end{aligned} \tag{17}$$

### Finite element solution

The previous form of the forward problem (16) can be directly discretized using finite element in space and finite difference in time in order to obtain a numerical solution to a particular set of initial and boundary conditions. Classically, the poroelastic system can be solved numerically in a fully coupled manner using  $(\mathbf{u}, p)$  as the main variables. This is the scheme programmed in Cast3M [17], the code used for all the numerical examples in this paper (for details see any finite element textbook such as Reference [18]).

Using an implicit finite difference scheme for time integration, one has to solve at each time step a linear system of equations

$$(\mathbf{K} - \Delta t_{n+1} \mathbf{P}) \mathbf{U}_{n+1} = \mathbf{K} \mathbf{U}_n + \mathbf{F}_{n+1} \tag{18}$$

where  $\mathbf{U}$  is the vector containing the nodal unknowns:  $\mathbf{U} = \begin{pmatrix} \mathbf{u} \\ p \end{pmatrix}$ . The subscripts  $n$  and  $n+1$  denote the known and unknown fields at time  $t_n$  and  $t_{n+1}$ , respectively.  $\mathbf{F}$  is the vector of applied forces. The boundary conditions involving the displacements and pore pressure are taken into account via Lagrange multipliers and are not represented here for the sake of simplicity.  $\mathbf{K}$  and  $\mathbf{P}$  denote, respectively, the poroelastic stiffness matrix and the permeability matrix.

$$\mathbf{K} = \int_{\Omega} \mathbf{D}^T \begin{bmatrix} \mathbf{C} & -\mathbf{b} \\ -\mathbf{b} & -1/M \end{bmatrix} \mathbf{D} \, dx, \quad \mathbf{P} = \int_{\Omega} \mathbf{E}^T \begin{bmatrix} 0 & 0 \\ 0 & \mathbf{K} \end{bmatrix} \mathbf{E} \, dx$$

where

$$\mathbf{D} = \begin{bmatrix} \mathbf{B} & 0 \\ 0 & \mathbf{N} \end{bmatrix}, \quad \mathbf{E} = \begin{bmatrix} 0 & 0 \\ 0 & \nabla \end{bmatrix}$$

The matrix  $\mathbf{B}$ ,  $\mathbf{N}$ ,  $\nabla$  are, respectively, the finite element approximation to the small strain operator, the shape function and the gradient matrix.

## THE INVERSE POROELASTIC PROBLEM $\mathcal{P}^{-1}$

A large number of inverse problems can be investigated in poroelasticity such as the identification of poroelastic constants (homogeneous, inhomogeneous, isotropic, anisotropic materials), the identification of unknown boundary conditions etc. Also several types of measurements during the time interval  $T = [0, t_f]$  can be considered: pore pressure, flux, stresses, displacements on the boundary or in points inside the domain.

We shall assume that the unknowns of the inverse problems can be reduced to a real vector denoted by  $\mathbf{m} = (m_1, \dots, m_i, \dots)$ . The solution of such inverse problems is then obtained by the

minimization of a cost functional with respect to  $\mathbf{m}$  measuring in some sense the mismatch between the measurements and the predictions obtained for a given set of parameters. In order to include all possible measurements, we can schematically write the cost functional as

$$\begin{aligned} \mathcal{J}(\mathbf{m}; \mathbf{u}, \boldsymbol{\sigma}, p, \mathbf{q}) = & \int_{\Gamma_i \times T} \varphi_1(\mathbf{u}) \, dx \, dt + \int_{\Gamma_u \times T} \varphi_2(\boldsymbol{\sigma} \cdot \mathbf{n}) \, dx \, dt + \int_{\Gamma_q \times T} \varphi_3(p) \, dx \, dt \\ & + \int_{\Gamma_p \times T} \varphi_4(\mathbf{q} \cdot \mathbf{n}) \, dx \, dt + \int_{\Omega \times T} \gamma(\mathbf{u}, p) \, dx \, dt \end{aligned} \quad (19)$$

where  $\varphi_1(\mathbf{u})$ ,  $\varphi_2(\boldsymbol{\sigma} \cdot \mathbf{n})$ ,  $\varphi_3(p)$ ,  $\varphi_4(\mathbf{q} \cdot \mathbf{n})$  and  $\gamma(\mathbf{u}, p)$  are functions of observations and predictions for a given value of the parameters  $\mathbf{m}$ . Typically, a simple least square form is used for  $\varphi$ , but other norms can be used. Note that, for boundary measurements, the displacements can be measured on the part where tensions are applied, pore pressure where flux is prescribed etc.

Also the functions can be viewed as distributions such that they take into account measurements on a smaller part of the boundary, or several points inside the domain. For example, the measurements may be recorded in a single point  $\mathbf{x}'$  in the domain. Therefore, we can define  $\gamma$  on the whole domain using the Dirac delta function.

This form of the cost functional (19) embodies all possible measurements on the boundary or inside the porous domain.

## THE DIRECT DIFFERENTIATION METHOD

Let us denote  $\delta_{m_i} \mathbf{u}$ ,  $\delta_{m_i} \zeta$ ,  $\delta_{m_i} \boldsymbol{\sigma}$  and  $\delta_{m_i} p$  as the first-order sensitivities with respect to the parameter  $m_i$  (i.e. the partial derivatives with respect to  $m_i$ ) of, respectively, the displacement field, the fluid content, the stresses and pore pressure. These sensitivity fields have the same tensorial rank as the original fields. They are solutions of a poroelastic problem with additional force terms depending on the solution of the direct problem. This problem, is obtained by simple differentiation with respect to  $m_i$  of the forward problem. In general,  $m_i$  can be any parameter entering the formulation of the original problem: loading, constitutive parameters, initial stresses. For simplicity, we do not consider the problem of shape parameters, the reader is referred to Reference [19] for more details regarding shape sensitivity.

### *Differentiated field equations*

The forward poroelastic problem is linear, its differentiation is therefore straightforward. We list the governing equations of the sensitivity problem.

- *Balance equation:*

$$\operatorname{div}(\delta_{m_i} \boldsymbol{\sigma}) + \frac{\partial \mathbf{F}}{\partial m_i} = \mathbf{0} \quad \text{in } \Omega \times T \quad (20)$$

- *Compatibility relation on  $\delta_{m_i} \mathbf{u}$ :*

$$\boldsymbol{\varepsilon}(\delta_{m_i} \mathbf{u}) = \frac{1}{2} (\nabla \delta_{m_i} \mathbf{u} + \nabla^T \delta_{m_i} \mathbf{u}) \quad \text{in } \Omega \times T \quad (21)$$



- *Fluid volume balance equation:*

$$\delta_{m_i} \dot{\zeta} + \frac{\partial g}{\partial m_i} = -\text{div } \delta_{m_i} \mathbf{q} \quad \text{in } \Omega \times T \quad (22)$$

- *Differentiated Darcy's law:*

$$\delta_{m_i} \mathbf{q} = -\mathbf{k} \cdot \left( \nabla \delta_{m_i} p - \frac{\partial \mathbf{f}}{\partial m_i} \right) - \frac{\partial \mathbf{k}}{\partial m_i} \cdot (\nabla p - \mathbf{f}) \quad \text{in } \Omega \times T \quad (23)$$

- *Differentiated constitutive relations:*

$$\begin{aligned} \delta_{m_i} \boldsymbol{\sigma} &= \mathbf{C}_u : \boldsymbol{\varepsilon}(\delta_{m_i} \mathbf{u}) - M \mathbf{b} \delta_{m_i} \zeta + \frac{\partial \mathbf{C}_u}{\partial m_i} : \boldsymbol{\varepsilon}(\mathbf{u}) - \frac{\partial M \mathbf{b}}{\partial m_i} \zeta \\ \delta_{m_i} p &= M(\delta_{m_i} \zeta - \mathbf{b} : \boldsymbol{\varepsilon}(\delta_{m_i} \mathbf{u})) + \frac{\partial M}{\partial m_i} \zeta - \frac{\partial M \mathbf{b}}{\partial m_i} : \boldsymbol{\varepsilon}(\mathbf{u}) \end{aligned} \quad (24)$$

The boundary conditions for the sensitivity problems become

$$\begin{aligned} \delta_{m_i} \boldsymbol{\sigma} \cdot \mathbf{n} &= \frac{\partial \mathbf{t}_g}{\partial m_i} \quad \text{on } \Gamma_t \times T \\ \delta_{m_i} \mathbf{u} &= \frac{\partial \mathbf{u}_g}{\partial m_i} \quad \text{on } \Gamma_u \times T \end{aligned} \quad (25)$$

and

$$\begin{aligned} \delta_{c_i} p &= \frac{\partial p_g}{\partial m_i} \quad \text{on } \Gamma_p \times T \\ \delta_{m_i} \mathbf{q} \cdot \mathbf{n} &= \frac{\partial q_g}{\partial m_i} \quad \text{on } \Gamma_q \times T \end{aligned} \quad (26)$$

*Initial conditions:* The initial conditions may eventually be a function of  $m_i$ . In that case, the equations that should satisfy the initial stresses and pore pressure fields (Equations (8) and (9)) have to be differentiated in order to obtain the corresponding initial sensitivities fields. The initial sensitivities stress field is the solution of the following boundary value problem:

$$\begin{aligned} \text{div}(\delta_{m_i} \boldsymbol{\sigma}_0) + \frac{\partial \mathbf{F}_0}{\partial c_i} &= \mathbf{0} \quad \text{in } \Omega \\ \delta_{m_i} \boldsymbol{\sigma}_0 \cdot \mathbf{n} &= \frac{\partial \mathbf{t}_g(0)}{\partial m_i} \quad \text{on } \Gamma_t \end{aligned} \quad (27)$$

and the pore pressure field is the solution of

$$\begin{aligned} \text{div} \left( \mathbf{k} \cdot \left( \nabla \delta_{m_i} p_0 - \frac{\partial \mathbf{f}_0}{\partial m_i} \right) \right) + \frac{\partial g_0}{\partial m_i} &= -\text{div} \left( \frac{\partial \mathbf{k}}{\partial m_i} \cdot (\nabla p_0 - \mathbf{f}_0) \right) \quad \text{in } \Omega \\ \delta_{m_i} \mathbf{q}_0 \cdot \mathbf{n} &= \frac{\partial q_g(0)}{\partial m_i} \quad \text{on } \Gamma_q \\ \delta_{m_i} p_0 &= \frac{\partial p_g(0)}{\partial m_i} \quad \text{on } \Gamma_p \end{aligned} \quad (28)$$

Similar to the forward problem, the initial sensitivities can be taken as a reference state and the unknown sensitivities for the evolution problem can be taken as variations from this initial state.

Equations (20)–(23) together with the initial conditions completely described the initial and boundary value problem on the sensitivities on parameter  $m_i$ . We can already notice that the difference between the original poroelastic problem and the sensitivity is very small. Only additional forces coming from the differentiation of the constitutive relations and the initial conditions appear. These force terms are functions of the solutions of the direct problem. In the case where  $m_i$  is a constitutive parameter, the initial and boundary conditions of the sensitivity problem are homogeneous, only the time-dependent force terms appear in the sensitivity problems.

### Weak form

The weak form of the sensitivity problem can be obtained directly from the previous strong formulation following the same lines as that for the forward problem. Taking  $\delta_{m_i}\mathbf{u}$  and  $\delta_{m_i}p$  as principal variables, we obtain

$$\begin{aligned} & \text{Find } \delta_{m_i}\mathbf{u} \in \delta_{m_i}\mathbf{U} \text{ and } \delta_{m_i}p \in \delta_{m_i}\mathbf{P} \text{ such that at all time } t \in T : \\ & \mathcal{E}(\delta_{m_i}\dot{\mathbf{u}}, \mathbf{v}) - \mathcal{C}(\delta_{m_i}\dot{p}, \mathbf{v}) - \mathcal{C}(r, \delta_{m_i}\dot{\mathbf{u}}) - \mathcal{S}(\delta_{m_i}\dot{p}, r) - \mathcal{A}(\delta_{m_i}(p - p_0), r) \\ & = \mathcal{C}_{\partial\mathbf{b}}(r, \dot{\mathbf{u}}) + \mathcal{S}_{\partial M}(\dot{p}, r) + \mathcal{A}_{\partial\mathbf{k}}(\delta_{m_i}(p - p_0), r) - \mathcal{E}_{\partial\mathbf{C}}(\dot{\mathbf{u}}, \mathbf{v}) + \mathcal{C}_{\partial\mathbf{b}}(\dot{p}, \mathbf{v}) \\ & + \int_{\Gamma_i} \mathbf{v} \frac{\partial \dot{\mathbf{i}}_g}{\partial m_i} dx + \int_{\Gamma_q} r \frac{\partial \mathbf{q}_g \cdot \mathbf{n}}{\partial m_i} dx + \int_{\Omega} \left( \mathbf{v} \frac{\partial \dot{\mathbf{F}}}{\partial m_i} + r \frac{\partial g}{\partial m_i} \right) dx \\ & \text{for all test fields } \mathbf{v} \in \mathbf{U}_0 \text{ and } r \in \mathbf{P}_0. \end{aligned}$$

The functional space  $\delta_{m_i}\mathbf{U}$  and  $\delta_{m_i}\mathbf{P}$  results simply from the differentiation of  $\mathbf{U}$  and  $\mathbf{P}$  with respect to  $m_i$

$$\begin{aligned} \delta_{m_i}\mathbf{U} &= \left\{ \delta_{m_i}\mathbf{u} \in H^1(\Omega) \mid \delta_{m_i}\mathbf{u} = 0 \text{ in } \Omega \text{ at } t = 0; \delta_{m_i}\mathbf{u} = \frac{\partial \mathbf{u}_g}{\partial m_i} \text{ on } \Gamma_u \times T \right\} \\ \delta_{m_i}\mathbf{P} &= \left\{ \delta_{m_i}p \in H^1(\Omega) \mid \delta_{m_i}p = \delta_{m_i}p_0 \text{ in } \Omega \text{ at } t = 0; \delta_{m_i}p = \frac{\partial p_g}{\partial m_i} \text{ on } \Gamma_p \times T \right\} \end{aligned}$$

The notation  $\mathcal{E}_{\partial\mathbf{C}}$  represents the following bi-linear operator:

$$\mathcal{E}_{\partial\mathbf{C}} = \int_{\Omega} \boldsymbol{\varepsilon}(\mathbf{u}) : \frac{\partial \mathbf{C}}{\partial m_i} : \boldsymbol{\varepsilon}(\mathbf{v}) dx \quad (29)$$

A similar notation is used for the other operators involving the partial derivatives with respect to the constitutive parameters such as  $\mathcal{A}_{\partial\mathbf{k}}$ ,  $\mathcal{S}_{\partial M}$ ,  $\mathcal{C}_{\partial\mathbf{b}}$ . Like for the direct problem, this form of the problem can be directly related to the numerical solution by finite element discretization in space and finite difference integration in time.

### Finite element solution

As already noticed, the forward and differentiated poroelastic problems are very similar. The difference lies only in the boundary conditions and the force terms in the differentiated problems, which directly depend on the solution of the forward problem. These features are

classic for a linear forward system of equations [7]. From a numerical stand point, the consequence is that, at each time step, only the right-hand side of the linear system will differ between the direct and differentiated problems. Therefore, the numerical solution of the differentiated and forward problems by finite elements in space and finite difference in time can be elegantly coupled and computational cost can be drastically reduced.

In order to have the same level of numerical accuracy for the differentiated and forward problems, the numerical solutions have to be consistent: same spatial and time discretization, same order of the finite elements [7, 20]. We always respected this recommendation in the numerical examples.

The DDM has been programmed using the object oriented finite element code `Cast3M`. The script language `Gibiane` allows a quick programming of the sensitivity problems. The linear system to solve at time  $t_{n+1}$  for the differentiated problem can be directly written from the weak form (29)

$$(\mathbf{K} - \Delta t_{n+1} \mathbf{P}) \delta_{m_i} \mathbf{U}_{n+1} = \mathbf{K} \delta_{m_i} \mathbf{U}_n + \frac{\partial \mathbf{F}_{n+1}}{\partial m_i} - \frac{\partial \mathbf{K}}{\partial m_i} (\mathbf{U}_{n+1} - \mathbf{U}_n) + \Delta t_{n+1} \frac{\partial \mathbf{P}}{\partial m_i} \mathbf{U}_{n+1} \quad (30)$$

We clearly see, that the global stiffness matrix  $(\mathbf{K} - \Delta t_{n+1} \mathbf{P})$  is equal to the one of the forward problem (18). Moreover, this matrix is the same for all differentiated problems as it does not depend on the parameter  $m_i$ . Only the right-hand side of the system has to be computed for each parameter  $m_i$ . The coupling between the numerical solution of the differentiated and forward will take advantage of this remark and use the LU decomposition of the matrix  $(\mathbf{K} - \Delta t_{n+1} \mathbf{P})$ . For one time step  $[t_n, t_{n+1}]$ , the scheme can be summarized as follows:

1. Solution of the forward problem at time  $t_{n+1}$ 
  - LU decomposition of the matrix  $(\mathbf{K} - \Delta t_{n+1} \mathbf{P})$ ,
  - Computation of the forces terms of Equation (18) (depending on  $\mathbf{U}_n$ ),
  - Solution of the linear system (18) to obtain  $\mathbf{U}_{n+1}$
2. Solution of the sensitivity problem on  $m_i$ 
  - Computation of the forces terms for the sensitivity problems (30) (depending on  $\mathbf{U}_{n+1}$ )
  - Solution of the linear system (30) via the stored LU decomposition of  $(\mathbf{K} - \Delta t_{n+1} \mathbf{P})$  to obtain  $\delta_{m_i} \mathbf{U}_{n+1}$ ,
3. The last step is repeated for the sensitivity problem on  $m_{i+1}$

We see that the sensitivity problems are thus solved in parallel with the forward problem. The use of a LU decomposition of the global matrix allow to greatly speed up the solution. Once the LU decomposition is known, the solution of the linear system is extremely fast as it only consists of basic operations. The additional cost of solving the  $p$  sensitivity problems on parameter  $m_i$  is extremely low if we use the LU decomposition of the stiffness matrix, which has to be computed only once. However the forces terms, different for each  $m_i$ , have to be computed.

The speed of the overall scheme will be even more reduced if a constant time step is used to solve the evolution problems in the interval  $T = [0, t_f]$ , as the LU decomposition can be passed from one time step to the other in that case.

In practice, the LU form of  $(\mathbf{K} - \Delta t_{n+1} \mathbf{P})$  is easily accessible while using the algorithm `pasapas` of the code `Cast3M` to solve the poroelastic problem. The use of personal routine `perso1` at the end of each time step allows to easily construct the forces terms for each sensitivity problems and to solve all the linear systems using the available LU decomposition of the global system matrices kept in memory.

*Case of the constitutive parameters:* In the case where one desires to obtain the sensitivities on the constitutive parameters, the computation of the forces terms involve the results of the forward problem as well as the different bi-linear operators derived with respect to the constitutive parameters like  $\mathcal{E}_{\partial C}$ . In the isotropic case, it is easier to use the following parameters  $\mathbf{m} = (E, \mu, b, M, k)$ . It is afterwards possible to switch to another set of poroelastic parameters using the different relations between them (see References [11, 1]) and the simple chain rule for differentiation of composed function. Using such a set of poroelastic parameters, we have simple expressions for the different differentiated bi-linear operators

$$\begin{aligned}\mathcal{E}_{\partial E} &= \frac{\mathcal{E}}{E}, & \mathcal{E}_{\partial \mu} &= \frac{\mathcal{E}}{\mu} \\ \mathcal{A}_{\partial k} &= \frac{\mathcal{A}}{k}, & \mathcal{C}_{\partial b} &= \frac{\mathcal{C}}{b} \\ \mathcal{S}_{\partial M} &= -\frac{\mathcal{S}}{M}\end{aligned}$$

Of course, we have  $\mathcal{E}_{\partial k} = 0$  etc. which greatly reduced the expressions of the sensitivity problems (29). We can note that, this procedure can also be applied to heterogeneous or anisotropic materials.

#### *Advantages and drawbacks of the method*

In comparison to a finite difference method, the DDM (DDM) provides an estimation of the sensitivities with the same level of accuracy as the solution of the forward problem. Also, the solution will always be stable in comparison to a finite difference estimation as it is independent of the choice of a differentiation step which is not the case for the finite difference method. Moreover, due to the efficient coupling between the sensitivities and the forward problem, the overall computational cost can be greatly reduced. We have found that in the case of the sensitivities on the 5 poroelastic parameters (homogeneous, isotropic case), the solution of the five additional sensitivity problems only increased the overall scheme by a factor of 1.2. In comparison, a finite difference scheme will cost the solution of six forward problems.

However, the DDM, even if the coupled scheme outlined above is used, is really efficient for a relatively small number of parameters (less than 20–30). If for example, in the case of a heterogeneous material, one wants to obtain an estimation of the sensitivities on the permeability at each nodes, the DDM is probably not very well suited. It will require the solution of large number of problems and a large amount of memory storage. In that particular case, the ASM will be better adapted.

## THE ADJOINT STATE METHOD

The adjoint state method (ASM) takes a different view on the minimization of the cost functional described in Equation (19). Especially, the implicit dependence of the solution of the forward problem upon the parameters  $\mathbf{m}$  is taken into account by stating that we face a constrained minimization problem:

Minimize  $\mathcal{J}(\mathbf{m}; \mathbf{u}, p, \boldsymbol{\sigma}, \mathbf{q})$  defined by equation (19) with respect to  $\mathbf{m}$  with the constraint that  $\mathbf{u}, p, \boldsymbol{\sigma}$  and  $\mathbf{q}$  are solutions of the forward problem  $\mathcal{P}$  Equation (16).

In the case of a constrained minimization problem, it is natural to introduce a Lagrangian  $\mathcal{L}$  by adjoining to the cost functional the weak form of the forward problem integrated in time on the interval of interest  $T$ :

$$\begin{aligned} \mathcal{L}(\mathbf{m}; \mathbf{u}, \boldsymbol{\sigma}, p, \mathbf{q}; \mathbf{u}^*, \boldsymbol{\sigma}^*, p^*, \mathbf{q}^*) &= \mathcal{J}(\mathbf{m}; \mathbf{u}, \boldsymbol{\sigma}, p, \mathbf{q}) \\ &+ \int_T (\mathcal{E}(\dot{\mathbf{u}}, \mathbf{u}^*) - \mathcal{C}(\dot{p}, \mathbf{u}^*) - \mathcal{C}(p^*, \dot{\mathbf{u}}) - \mathcal{S}(\dot{p}, p^*) - \mathcal{A}(p - p_0, p^*)) dt \\ &- \int_T \int_{\Gamma} \mathbf{u}^* \cdot (\boldsymbol{\sigma} \cdot \mathbf{n}) dx dt - \int_T \int_{\Gamma} p^* \mathbf{q} \cdot \mathbf{n} dx dt \end{aligned} \quad (31)$$

All variables are supposed to be mutually independent. The virtual displacement  $\mathbf{u}^*$  and virtual pore pressure  $p^*$  play the role of Lagrange multiplier (denoted adjoint variables hereafter). The construction of this Lagrangian ensures that its saddle point gives the minimum of the cost functional with  $\mathbf{u}$  and  $p$  solution of the forward problem:

If  $(\mathbf{u}, \boldsymbol{\sigma}, p, \mathbf{q})$  are solution of the forward problem  $\mathcal{P}$  then  $\mathcal{J} \equiv \mathcal{L}$

An adjoint poroelastic problem has already been derived and used in the context of the boundary element method to solve the poroelastic forward problem [21]. The poroelastic system of equation is not self-adjoint due to the presence of the diffusivity equation. In the following, we re-derive the adjoint problem following the lines of optimal control [22], having in mind the estimation of the gradient of the cost functional  $\mathcal{J}$  (19) with respect to the parameters  $\mathbf{m}$ .

### *The adjoint problem*

All variables being mutually independent, the stationarity conditions of the Lagrangian can be formally written as follows:

$$\left( \frac{\partial \mathcal{L}}{\partial \mathbf{u}^*}, \mathbf{du}^* \right) = \int_T (\mathcal{E}(\dot{\mathbf{u}}, \mathbf{du}^*) - \mathcal{C}(\dot{p}, \mathbf{du}^*)) dt - \int_T \int_{\Gamma} \mathbf{du}^* \boldsymbol{\sigma} \cdot \mathbf{n} dx dt = 0 \quad (32)$$

$$\begin{aligned} \left( \frac{\partial \mathcal{L}}{\partial p^*}, dp^* \right) &= - \int_T (\mathcal{C}(dp^*, \dot{\mathbf{u}}) + \mathcal{S}(\dot{p}, dp^*) + \mathcal{A}(p - p_0, dp^*)) dt \\ &- \int_T \int_{\Gamma} dp^* \mathbf{q} \cdot \mathbf{n} dx dt = 0 \end{aligned} \quad (33)$$

$$\begin{aligned} \left( \frac{\partial \mathcal{L}}{\partial \mathbf{u}}, \mathbf{d}\mathbf{u} \right) &= \int_{\Gamma_i \times T} \partial_{\mathbf{u}} \varphi_1(\mathbf{u}) \mathbf{d}\mathbf{u} \, dx \, dt + \int_{\Omega \times T} \partial_{\mathbf{u}} \gamma(\mathbf{u}, p) \mathbf{d}\mathbf{u} \, dx \, dt \\ &\quad + \int_T (\mathcal{E}(\mathbf{d}\dot{\mathbf{u}}, \mathbf{u}^*) - \mathcal{C}(p^*, \mathbf{d}\dot{\mathbf{u}})) \, dt = 0 \end{aligned} \quad (34)$$

$$\begin{aligned} \left( \frac{\partial \mathcal{L}}{\partial p}, dp \right) &= \int_{\Gamma_q \times T} \partial_p \varphi_3(p) \, dp \, dx \, dt + \int_{\Omega \times T} \partial_p \gamma(\mathbf{u}, p) \, dp \, dx \, dt \\ &\quad - \int_T (\mathcal{C}(\mathbf{d}\dot{p}, \mathbf{u}^*) + \mathcal{S}(\mathbf{d}\dot{p}, p^*) + \mathcal{A}(dp, p^*)) \, dt = 0 \end{aligned} \quad (35)$$

$$\left( \frac{\partial \mathcal{L}}{\partial \boldsymbol{\sigma}}, \mathbf{d}\boldsymbol{\sigma} \right) = \int_{\Gamma_u \times T} \partial_{\boldsymbol{\sigma}} \varphi_2(\boldsymbol{\sigma}) \mathbf{d}\boldsymbol{\sigma} \cdot \mathbf{n} \, dx \, dt - \int_{\Gamma \times T} \mathbf{u}^* \mathbf{d}\boldsymbol{\sigma} \cdot \mathbf{n} \, dx \, dt = 0 \quad (36)$$

$$\left( \frac{\partial \mathcal{L}}{\partial \mathbf{q}}, \mathbf{d}\mathbf{q} \right) = \int_{\Gamma_p \times T} \partial_{\mathbf{q}} \varphi_4(\mathbf{q} \cdot \mathbf{n}) \mathbf{d}\mathbf{q} \cdot \mathbf{n} \, dx \, dt - \int_{\Gamma \times T} p^* \mathbf{d}\mathbf{q} \cdot \mathbf{n} \, dx \, dt = 0 \quad (37)$$

The stationarity conditions with respect to the adjoint variables (32) and (33) returns the weak form of the direct poroelastic problem (16).

The stationarity conditions on the direct variables, after integration by part in time of Equations (34)–(37), furnish the following weak form of the adjoint problem on the variables  $(\mathbf{u}^*, p^*)$ :

Find  $\mathbf{u}^* \in \mathbf{U}^*$  and  $p^* \in \mathbf{P}^*$  such that at all time  $t \in T$  :

$$\begin{aligned} &\mathcal{E}(\dot{\mathbf{u}}^*, \mathbf{v}) - \mathcal{C}(p^*, \mathbf{v}) - \mathcal{C}(r, \dot{\mathbf{u}}^*) - \mathcal{S}(\dot{p}^*, r) + \mathcal{A}(p^*, r) \\ &= \int_{\Gamma_i} \mathbf{v} \partial_{\mathbf{u}} \varphi_1(\mathbf{u}) \, dx + \int_{\Gamma_q} r \partial_p \varphi_3(p) \, dx + \int_{\Omega} (\mathbf{v} \partial_{\mathbf{u}} \gamma(\mathbf{u}, p) + r \partial_p \gamma(\mathbf{u}, p)) \, dx \end{aligned} \quad (38)$$

for all test fields  $r \in \mathbf{P}_f^*$  and  $\mathbf{v} \in \mathbf{U}_f^*$ .

where the adjoint functional spaces, incorporating the final conditions, are defined as follows:

$$\mathbf{U}^* = \{ \mathbf{u}^* \in H^1(\Omega) \mid \mathbf{u}^* = 0 \text{ in } \Omega \text{ at } t = t_f; \dot{\mathbf{u}}^* = -\partial_{\boldsymbol{\sigma}} \varphi_2(\boldsymbol{\sigma}) \text{ on } \Gamma_u \times T \}$$

$$\mathbf{P}^* = \{ p^* \in H^1(\Omega) \mid p^* = 0 \text{ in } \Omega \text{ at } t = t_f; p^* = \partial_{\mathbf{q}} \varphi_4(\mathbf{q} \cdot \mathbf{n}) \text{ on } \Gamma_p \times T \}$$

$$\mathbf{U}_f^* = \{ \mathbf{v} \in H^1(\Omega) \mid \mathbf{v} = 0 \text{ in } \Omega \text{ at } t = t_f; \mathbf{v} = 0 \text{ on } \Gamma_u \times T \}$$

$$\mathbf{P}_f^* = \{ r \in H^1(\Omega) \mid r = 0 \text{ in } \Omega \text{ at } t = t_f; r = 0 \text{ on } \Gamma_p \times T \}$$

### Gradient of the cost functional

For a given point  $\mathbf{m}$ , if  $(\mathbf{u}, p)$  are solutions of the direct problem  $(\mathcal{P})$ , by definition of the Lagrangian  $\mathcal{L}$ , we have  $\mathcal{L} \equiv \mathcal{J}$ . Moreover, if  $(\mathbf{u}^*, p^*)$  are solutions of the adjoint problem  $\mathcal{P}^a$  (38) previously described, we obtain:

$$\nabla_{\mathbf{m}} \mathcal{J} = \nabla_{\mathbf{m}} \mathcal{L} \quad (39)$$

In the case of constitutive parameters, i.e.  $\mathbf{m} = (\mathbf{C}, \mathbf{b}, \mathbf{k}, M)$ , one obtains the following components for  $\nabla_{\mathbf{m}}\mathcal{J}$ :

$$\begin{aligned}\frac{\partial \mathcal{J}}{\partial \mathbf{C}} &= \int_T \mathcal{E}_{\partial \mathbf{C}}(\dot{\mathbf{u}}, \mathbf{u}^*) \, dt \\ \frac{\partial \mathcal{J}}{\partial \mathbf{b}} &= - \int_T \mathcal{E}_{\partial \mathbf{b}}(\dot{p}, \mathbf{u}^*) \, dt - \int_T \mathcal{E}_{\partial \mathbf{b}}(p^*, \dot{\mathbf{u}}) \, dt \\ \frac{\partial \mathcal{J}}{\partial M} &= - \int_T \mathcal{S}_{\partial M}(\dot{p}, p^*) \, dt \\ \frac{\partial \mathcal{J}}{\partial \mathbf{k}} &= - \int_T \mathcal{A}_{\partial \mathbf{k}}(p - p_0, p^*) \, dt\end{aligned}$$

where  $\mathcal{E}_{\partial \mathbf{C}}$  denotes the partial derivative of the elasticity operator with respect to the elastic moduli  $\mathbf{C}$  as defined in Equation (29). The same notation holds for the others operators.

Therefore, in order to compute the gradient of the cost functional  $\nabla_{\mathbf{m}}\mathcal{J}$ , one needs to solve both the forward  $\mathcal{P}$  and adjoint problems  $\mathcal{P}^a$ .

#### *Strong form of the adjoint problem*

Knowing the definition of the bilinear operators, Equations (12)–(15), it is straightforward to deduce from the weak form of the adjoint problem  $\mathcal{P}^a$  (38) the corresponding strong form.

- *Final conditions:*

$$\begin{aligned}\operatorname{div} \boldsymbol{\sigma}^*(t_f) &= \mathbf{0} \quad \text{in } \Omega \\ \boldsymbol{\sigma}^*(t_f) \cdot \mathbf{n} &= 0 \quad \text{on } \Gamma_t\end{aligned}\tag{40}$$

$$\begin{aligned}\mathbf{u}^*(t_f) &= 0 \quad \text{in } \Omega \\ p^*(t_f) &= 0 \quad \text{on } \Omega\end{aligned}\tag{41}$$

- *Equilibrium, compatibility and fluid balance equations:*

$$\begin{aligned}\operatorname{div} \boldsymbol{\sigma}^* + \partial_{\mathbf{u}}\gamma(\mathbf{u}, p) &= \mathbf{0} \quad \text{in } \Omega \times T \\ \boldsymbol{\varepsilon}(\dot{\mathbf{u}}^*) &= \frac{1}{2}(\nabla \dot{\mathbf{u}}^* + \nabla^T \dot{\mathbf{u}}^*) \quad \text{in } \Omega \times T \\ \dot{\zeta}^* + \partial_p \gamma(\mathbf{u}, p) &= -\operatorname{div} \mathbf{q}^* \quad \text{in } \Omega \times T\end{aligned}\tag{42}$$

- *Boundary conditions:*

$$\begin{aligned}\boldsymbol{\sigma}^* \cdot \mathbf{n} &= \partial_{\mathbf{u}}\varphi_1(\mathbf{u}) \quad \text{in } \Gamma_t \times T \\ p^* &= \partial_{\mathbf{q}}\varphi_4(\mathbf{q} \cdot \mathbf{n}) \quad \text{in } \Gamma_p \times T \\ \dot{\mathbf{u}}^* &= -\partial_{\boldsymbol{\sigma}}\varphi_2(\boldsymbol{\sigma}) \quad \text{in } \Gamma_u \times T \\ \mathbf{q}^* \cdot \mathbf{n} &= \partial_p\varphi_3(p) \quad \text{in } \Gamma_q \times T\end{aligned}\tag{43}$$

- *Adjoint transport law:*

$$q^* = \mathbf{k} \nabla p^* \quad \text{in } \Omega \times T\tag{44}$$

- *Adjoint poroelastic constitutive law:*

$$\begin{aligned}\dot{\boldsymbol{\sigma}}^* &= (\mathbf{C} + \mathbf{b} \otimes \mathbf{b}M)\boldsymbol{\varepsilon}(\dot{\mathbf{u}}^*) - M\dot{\boldsymbol{\zeta}}^* \quad \text{in } \Omega \times T \\ \dot{p}^* &= M(\dot{\boldsymbol{\zeta}}^* - \mathbf{b} : \boldsymbol{\varepsilon}(\dot{\mathbf{u}}^*)) \quad \text{in } \Omega \times T\end{aligned}\tag{45}$$

We clearly see that the differences between the direct and adjoint problems lie in the final and boundary conditions as well as the transport law (44).

The classical expression of Darcy's law (4) is replaced by the adjoint form (44). This change of sign together with the final conditions at  $t = t_f$  explain the backward character in time of the adjoint poroelastic system.

### *Finite element solution*

As noticed previously, the adjoint problem is a backward poroelastic problem with a final condition instead of an initial one. After a change of variables:  $t^* = t - t_f$ , the problem is strictly similar to a direct poroelastic problem. The boundary and final conditions of this problem depend on the solution of the direct problem. Therefore, the adjoint poroelastic problem is solved after the solution of the direct problem has been obtained. Moreover, the boundary conditions at time  $t^*$  are computed from the solution of the direct problem at  $t^*$ .

The gradient of the cost functional is computed using Equation (40), after the solutions of the direct and adjoint problems have been obtained. We recall that the local sensitivities of the poromechanical fields are not obtained with the ASM but the gradient of the cost functional is computed only via the solution of two poroelastic problems independently of the number of unknowns parameters  $\mathbf{m}$ .

It is important to note that passing from the direct to the adjoint problem changes the integration scheme from implicit (forward Euler) to explicit (backward Euler) and vice versa. This particularity has to be taken into account in the choice of the evolution of the time step [7].

## NUMERICAL EXAMPLES

### *Hollow sphere under oscillatory internal pressure*

As a first example to test the DDM and ASM, we consider the problem of a hollow poroelastic sphere of internal radius  $R_i = 1$  and external radius  $R_e = 2.5$ . Its inner surface is subjected to an oscillatory pressure and pore pressure

$$\boldsymbol{\sigma}(t) \cdot \mathbf{n} = H \sin(\omega t)$$

$$p(t) = H \sin(\omega t)$$

The outer surface is undrained and free of traction.

The radial displacement produced by this loading is supposed to be measured on the outer surface. As a consequence we dispose of overspecified boundary conditions and can define the following cost functional:

$$\mathcal{J}(\mathbf{m}) = \int_T \frac{1}{2} (u_{r_{\text{measured}}}(t) - u_r(\mathbf{m}, t))^2 dt\tag{46}$$



On the one hand, we shall compare the sensitivities obtained by DDM and a finite difference scheme and, on the other hand, we shall compute the gradient of a mismatch cost functional using the DDM, ASM and finite difference.

Although the problem is clearly one-dimensional for a homogeneous material as subject to spherical symmetry, we solve it numerically by the finite element method using a bi-dimensional mesh under axial symmetry. The computation is performed with the following material constants (Table I):

$$E = 9.36 \text{ GPa}, \quad \nu = 0.2, \quad M = 18.6 \text{ GPa}$$

$$b = 0.83, \quad \kappa = 0.2 \cdot 10^{-9} \text{ m}^2, \quad \mu_f = 10^3 \text{ Pa s}$$

Figure 2 shows the evolution of the pore pressure and radial displacement on the inner and outer surface. The corresponding sensitivity coefficients are displayed in Figure 3. Table II presents the numerical values of the sensitivities obtained by DDM and finite difference. The values are equal up to three digits.

The comparisons of the gradient of  $\mathcal{J}$  defined in Equation (46) is obtained by the three methods in a particular point and is presented in the Table I. We remark, that the values are in excellent agreement.

Table I. Comparison of the functional gradient (hollow sphere example) for  $E = 14.04 \text{ GPa}$ ,  $M = 18.06 \text{ GPa}$ ,  $b = 0.7$ ,  $k = 2.65 \times 10^{-9} \text{ m}^2$  and  $\mu_f = 10^3 \text{ Pa s}$ .

	FD	DDM	ASM
$\mathcal{J}$	1.81201E-02	1.81201E-02	1.81201E-02
$\nabla_E \mathcal{J}$	2.58636E-02	2.57086E-02	2.50994E-02
$\nabla_b \mathcal{J}$	8.46560E-03	8.38752E-03	8.3184E-03
$\nabla_M \mathcal{J}$	6.27311E-05	6.22351E-05	6.2802E-05

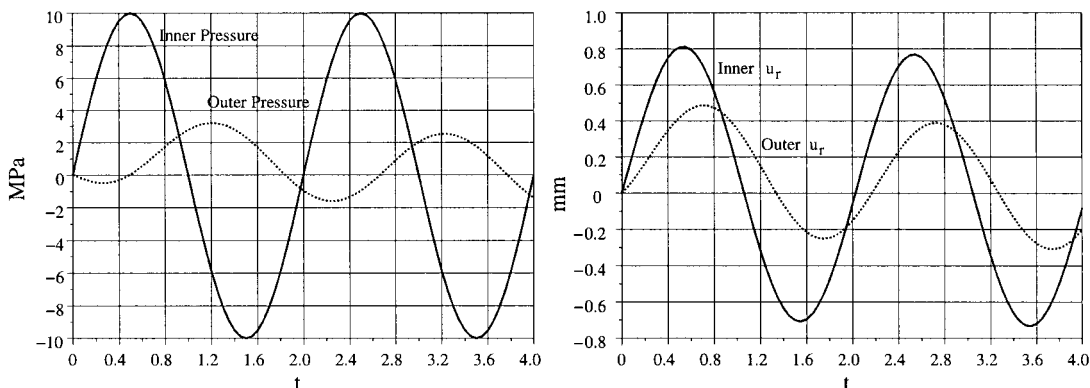


Figure 2. Time evolution of pore pressure and radial displacement on the inner and outer surface of the hollow sphere (first example).

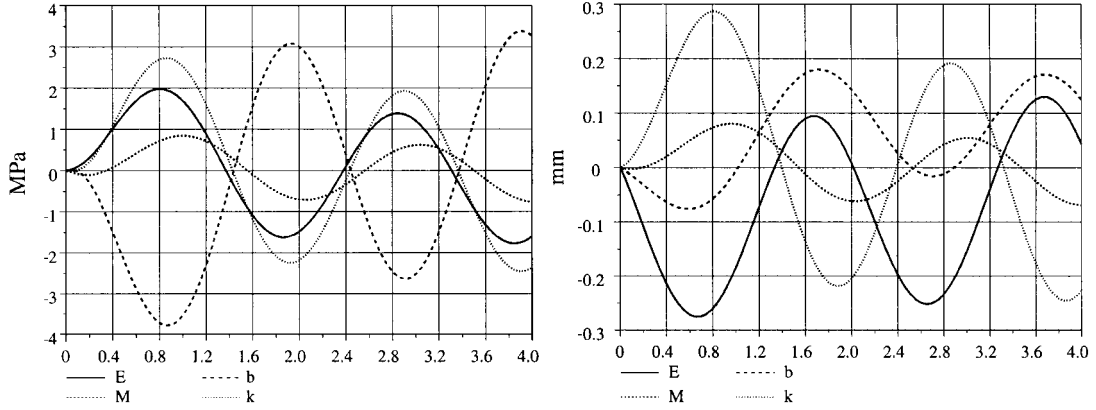


Figure 3. Time evolution of the sensitivities coefficient of the outer pore pressure (left panel) and of the radial displacement (right panel) ( $m_i \delta_{m_i} u_r(r = R_e, t)$ ) for the hollow sphere (first example).

Table II. Comparison finite difference and direct differentiation for  $E = 14.04$  GPa,  $M = 18.06$  GPa,  $b = 0.7$ ,  $k = 2.65 \times 10^{-9}$  m<sup>2</sup> (hollow sphere, first example).

Time	$E \delta_E u_r(r = R_e) \text{ 1e-3}$		$M \delta_M u_r(r = R_e) \text{ 1e-4}$		$b \delta_b u_r(r = R_e) \text{ 1e-3}$		$k \delta_k u_r(r = R_e) \text{ 1e-3}$	
	FD	DDM	FD	DDM	FD	DDM	FD	DDM
0.4	-0.663765	-0.664143	0.565540	0.568142	0.459273	0.459000	0.128135	0.128733
0.8	-0.672403	-0.672833	-0.259502	-0.257120	0.618375	0.617754	-0.062605	-0.062044
1.2	0.233582	0.233676	-0.808950	-0.810130	-0.052898	-0.053079	-0.184853	-0.185125
1.6	0.816166	0.816659	-0.244495	-0.247614	-0.650004	-0.649504	-0.052508	-0.053241
2	0.270814	0.271031	0.657686	0.656939	-0.348786	-0.348301	0.152367	0.152186
2.4	-0.648794	-0.649147	0.650962	0.653618	0.434443	0.434238	0.146675	0.147296
2.8	-0.671792	-0.672221	-0.255369	-0.252980	0.617287	0.616671	-0.061716	-0.061152
3.2	0.233604	0.233698	-0.808789	-0.809970	-0.052939	-0.053119	-0.184818	-0.185091
3.6	0.816167	0.816660	-0.244489	-0.247608	-0.650005	-0.649505	-0.052507	-0.053239
4	0.270815	0.271031	0.657686	0.656939	-0.348786	-0.348301	0.152367	0.152187

### Hollow cylinder under complex loading

Let us now consider the case of a hollow cylinder of inner radius  $R_i = 1$  and outer radius  $R_e = 2.5$  as displayed in Figure 4. A constant pore pressure  $p = \pi$  is applied to a part of the inner radial surface while the rest of this surface remains undrained during the time of interest  $[0, t_f]$ . The top and bottom surface are drained, whereas the outer radial surface is undrained. A variable mechanical pressure (compression) is applied at the top of the cylinder. Figure 5 displays the evolution of the applied pressure as well as the corresponding evolution of the vertical displacement of the top platten.

We can note the delayed displacement due to the poroelastic coupling. The stresses contour at a given time during the transient phase are displayed on Figure 6. The two-dimensional effect due to the hydraulic loading is clearly visible.

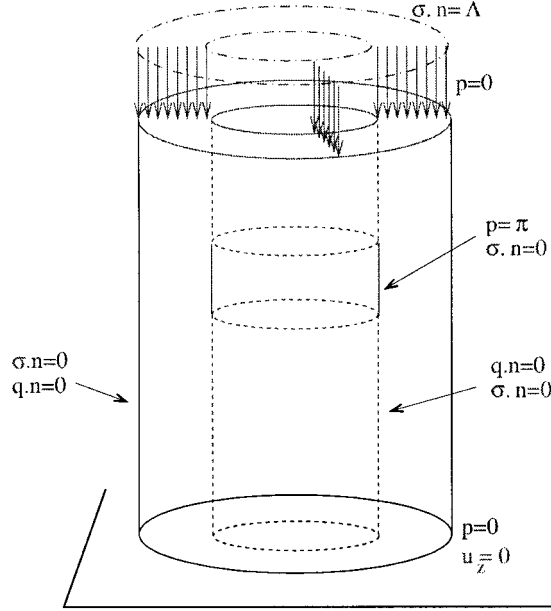


Figure 4. Schematic view of the configuration of the hollow cylinder example (second example).

The contour of the sensitivities of the stresses on the Biot modulus at the middle of the loading are shown on Figure 7. Similar patterns can be observed for the other parameters.

#### *Identification of some poroelastic coefficients*

As an application, we will seek to recover some poroelastic parameters from the knowledge of the vertical displacement of the top platten for the hollow cylinder example described in the previous section. The measurements are simulated by a preliminary simulation and perturbed with 3% of white noise. The chosen values of the poroelastic parameters that we will try to recover from the data are

$$\begin{aligned}
 E &= 4.5 \text{ GPa}, \quad \nu = 0.2, \quad M = 30 \text{ MPa} \\
 b &= 0.658, \quad k = 3 \times 10^{-11} \text{ m}^2 \text{ Pa}^{-1} \text{ s}^{-1}
 \end{aligned}
 \tag{47}$$

The identification is formulated as the minimization of the following cost functional:

$$\mathcal{J}(\mathbf{m}) = \frac{1}{2} \int_{\Gamma_{\text{sup}}} \int_T (u_z(\mathbf{m}, t) - u_{z_{\text{data}}}(t))^2 dx dt$$

where  $u_{z_{\text{data}}}(t)$  are the simulated data of the vertical displacement and  $u_z(\mathbf{m}, t)$  are the corresponding predictions for a given set of poroelastic parameters  $\mathbf{m}$  (Figure 8).

In this case, we only try to retrieve the value of the Biot coefficient  $b$ , hydraulic conductivity  $k$  and drained young modulus  $E$  from the displacement data. The optimization is performed using a gradient based algorithm. We will use the two methods (ASM and DDM) in order to obtain the gradient components: direct differentiation coupled with a Levenberg–Marquardt

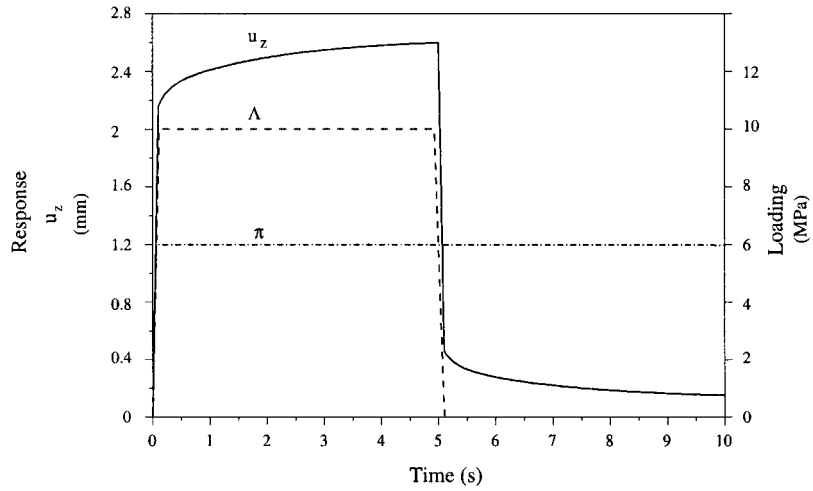


Figure 5. Loading path for the applied stresses  $\Lambda$  and the pore pressure  $\pi$  together with the induced vertical displacement  $u_z$  (second example).

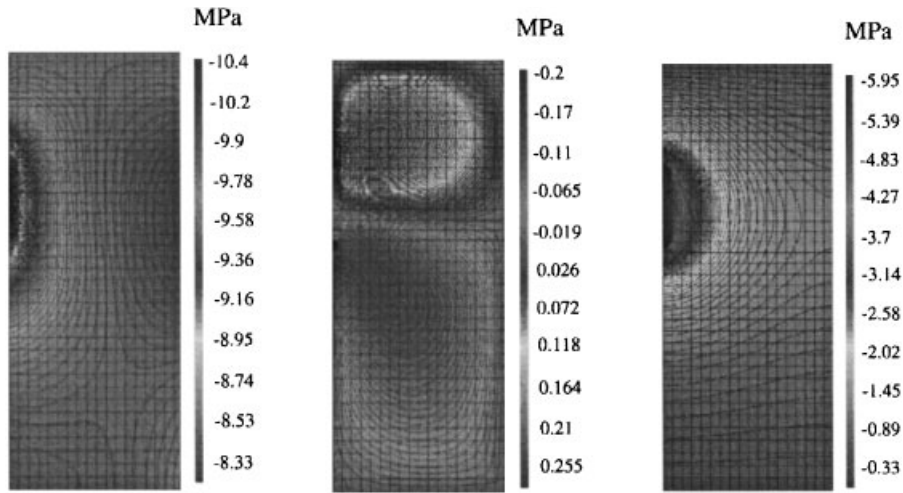


Figure 6. Contour of  $\sigma_{zz}$ ,  $\sigma_{rz}$ ,  $p$  at the middle of the transient phase (axisymmetrical modelling, second example).

algorithm and the adjoint state coupled with a BFGS update of the Hessian and a Wolfe line search. For a general review of numerical minimization algorithms, see References [23, 24].

Several optimizations starting from different guesses for the initial values of the unknown parameters have been performed. The results are summarized, respectively, in Tables III and IV for the case of the DDM and ASM, respectively. We can see that we always recover the

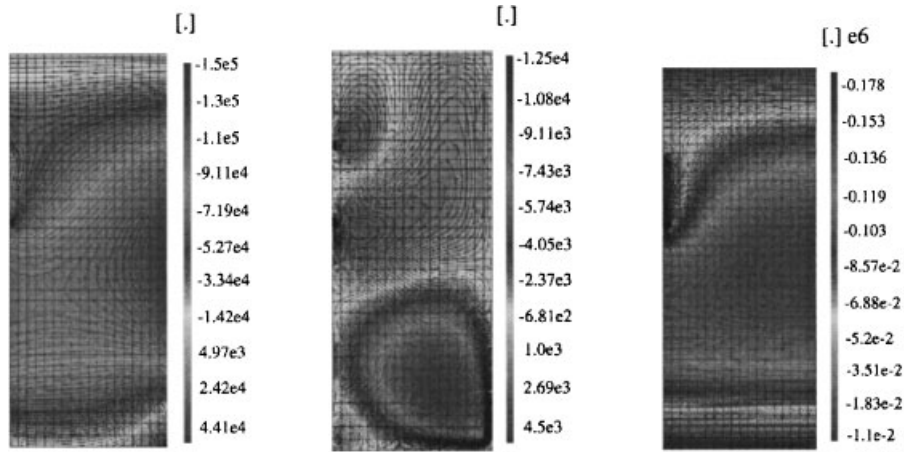


Figure 7. Corresponding contour of  $\delta_M \sigma_{zz}$ ,  $\delta_M \sigma_{rz}$ ,  $\delta_M p$  at the middle of the transient phase (axisymmetrical modelling, second example).

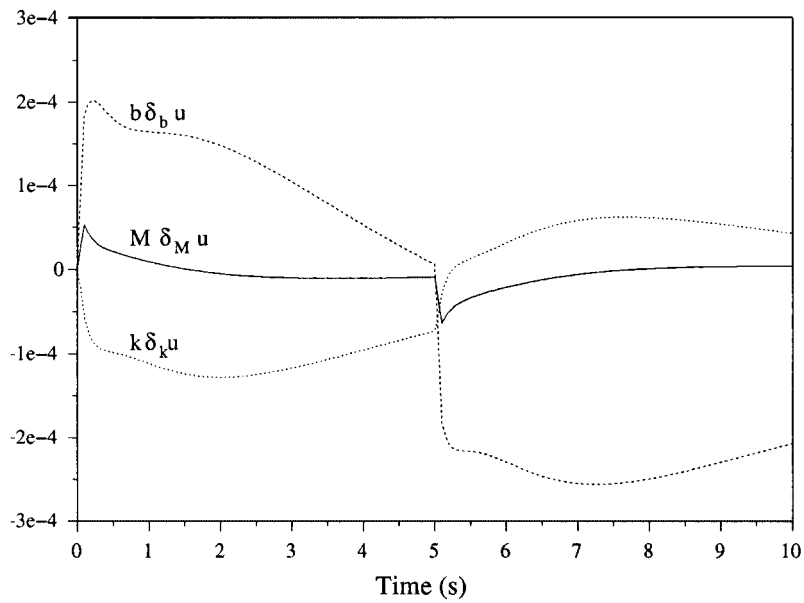


Figure 8. Evolution of the sensitivity coefficient of the vertical displacement on different parameters obtained by Direct differentiation (hollow cylinder, second example).

optimum values of the parameters (47). We can also note that in the case where the optimization is performed using a Levenberg–Marquardt algorithm with the sensitivities computed by DDM, the convergence was always reached within 15 iterations. The evolution of the estimated parameters during an optimization process in that case is displayed in Figure 9.

Table III. Identification results, gradient by direct differentiation and Levenberg–Marquardt algorithm.

	$E$ (GPa)	$k$ ( $\times 10^{-10}$ m <sup>2</sup> Pa <sup>-1</sup> s <sup>-1</sup> )	$b$
Initial	5	0.1	0.2
Identified	4.5	0.2997471	0.6580478
Initial	2	0.6	0.2
Identified	4.51	0.3292477	0.6859921
Initial	6.0	0.8	0.8
Identified	4.5	0.3003186	0.6585730
Initial	8.0	0.09	0.3
Identified	4.499	0.2986915	0.657082
Optimum	4.5	0.3	0.658

Table IV. Identification results, gradient by the ASM and BFGS type algorithm.

	$E$ (GPa)	$k$ ( $\times 10^{-10}$ m <sup>2</sup> Pa <sup>-1</sup> s <sup>-1</sup> )	$b$
Initial	5	0.1	0.2
Identified	4.487	0.25835	0.65573
Initial	2	0.6	0.2
Identified	4.512	0.34512	0.6654
Initial	6.0	0.8	0.8
Identified	4.485	0.3245	0.6734
Initial	8.0	0.09	0.3
Identified	4.49	0.2867	0.6578
Optimum	4.5	0.3	0.658

The results obtained via the ASM for the estimate of the cost functional gradient and a BFGS scheme are slightly less precise as one can notice on Table IV. The convergence is also slightly slower. Nevertheless, we recover the optimum parameters (47).

## CONCLUSIONS

We have extended the DDM and ASM to the case of quasi-static linear poroelasticity and discussed their finite element programming. Their efficiency in computing sensitivities and gradients of cost functionals has been illustrated using two numerical examples. The examples also showed the possibility of applying these techniques for parameter identification problems.

The importance of these techniques lies in their accuracy and computational efficiency in comparison to any finite difference scheme. It is also important to notice, that their introduction into existing finite element codes does impose only a small amount of additional programming, provided the codes have an open architecture. Moreover, the present formulation can be further

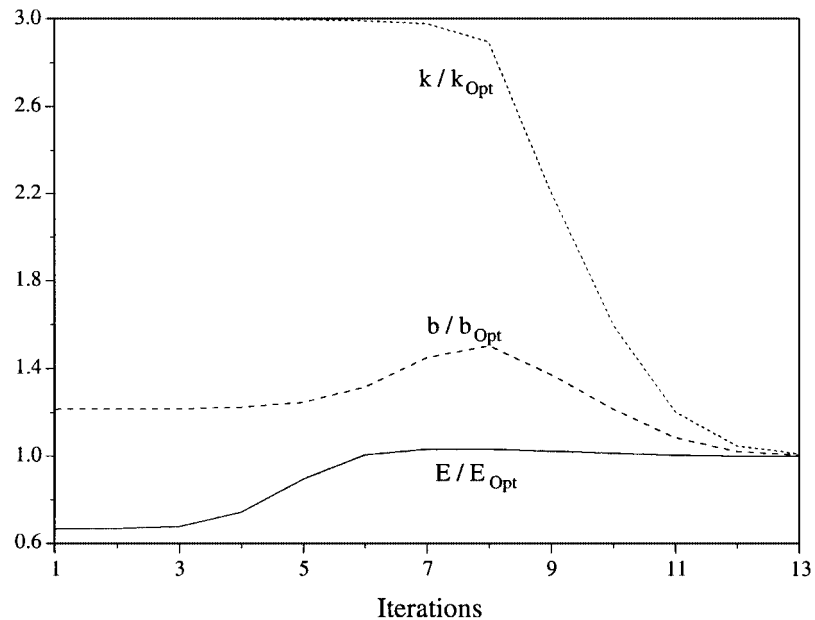


Figure 9. Convergence of the parameters toward their optimal values (gradient by DDM).

extended to other coupled problems such as thermo-poro-elasticity, or nonlinear constitutive behaviours such as poro-viscoplasticity.

From a practical point of view, we recall that parameter identification problems are generally ill posed, i.e. uniqueness and stability of the solution with respect to initial data are not assured. Therefore in the application of the preceding techniques further precautions have to be taken. As a rule of thumb, a complete dimensional analysis of the particular forward problem must be conducted in order to obtain the lumped parameters that have an influence on the measured quantity. Nonetheless, such dimensional analysis will only give the maximum number of parameters entering in the system response. It will not avoid the less obvious non-uniqueness problems. To our knowledge the question of uniqueness of the parameter identification problem in poroelasticity with respect to the available measurements is still an open question to be addressed in the future.

#### ACKNOWLEDGEMENT

Part of this work has been done during the PhD of B. L. at LMS, Ecole Polytechnique, France [25], sponsored by the French Agency for Radioactive Waste Management (ANDRA).

#### REFERENCES

1. Detournay E, Cheng AHD. *Fundamentals of Poroelasticity*, *Comprehensive Rocks Engineering*, vol. 2, Chapter 5. Pergamon: New York, 1993.

2. Wang HF. *Theory of Linear Poroelasticity with Applications to Geomechanics and Hydrogeology*. Princeton University Press: Princeton, NJ, 2000.
3. Cowin SC. Bone poroelasticity. *Journal of Biomechanics* 1999; **32**:217–238.
4. Lecampion B, Constantinescu A, Malinsky L. Identification of poroelastic constants of tight rocks from laboratory tests. *International Journal of Geomechanics* 2004, submitted.
5. Detournay E, Berchenko I. Thermoporoelastic experiments at url. *International Journal of Rock Mechanics and Mining Sciences* 2004; **12**:155–164.
6. Constantinescu A. Identification and inverse problems in solid mechanics. In *A Global Computational Approach in Engineering Problems: Identification and Fatigue*, number Lecture note 8 in AMAS. Institute of Fundamental Technological Research, 2004.
7. Tortorelli DA, Michaleris P. Design sensitivity analysis: overview and review. *Inverse Problems in Engineering* 1994; **1**:71–103.
8. Mahnken R, Steinmann P. A finite element algorithm for parameter identification of material models for fluid saturated porous media. *International Journal for Numerical and Analytical Methods in Geomechanics* 2001; **25**: 415–434.
9. Bonnet M, Bui HD, Maigre H, Planchard J. Identification of heat conduction coefficient: application to nondestructive testing. In *IUTAM Symposium on Inverse Problems in Engineering Mechanics*, Bui HD, Tanaka M (eds). Springer: Tokyo, 1992.
10. Dems K, Mróz Z. Variational approach to sensitivity analysis in thermoelasticity. *Journal of Thermal Stresses* 1987; **10**:283–306.
11. Coussy O. *Poromechanics*. Wiley: New York, 2004.
12. Cheng AHD, Liggett JA. Boundary integral equation method for linear poroelasticity with applications to soil consolidation. *International Journal for Numerical Methods in Engineering* 1984; **20**:255–278.
13. Cheng AHD, Predeleanu M. Transient boundary element formulation in poroelasticity. *Applied Mathematical Modelling* 1987; **11**:285–290.
14. Curran JH, Carvalho JL. A displacement discontinuity model for fluid-saturated porous media. In *Proceedings of the 6th Congress of International Society of Rock Mechanics*, vol. 1. Montreal, 1987; 73–78.
15. Biot MA. General theory of three-dimensional consolidation. *Journal of Applied Physics* 1941; **12**:155–164.
16. Biot MA. Theory of elasticity and consolidation for a porous anisotropic solid. *Journal of Applied Physics* 1955; **26**:182–185.
17. CEA. Cast3m, a finite element solver. Available online for research and education, 2003. <http://www-cast3m.cea.fr>.
18. Zienkiewicz OC. *The Finite Element Method*. Mc-Graw Hill: New York, 1977.
19. Arora JS, Cardoso JB. Variational principle for shape sensitivity analysis. *AIAA Journal* 1992; **30**:538–547.
20. Vidal CA, Lee HS, Haber RB. The consistent tangent operator for design sensitivity analysis of history-dependent response. *Computing Systems in Engineering* 1991; **2**(5/6):509–523.
21. Predeleanu M. Reciprocal theorem in the consolidation theory of porous media. *Anal. Univ. Bucuresti, Seria Stiintele Naturii, Matematica, Mecanica* 1968; **17**:75–79.
22. Lions JL. *Contrôle optimal des équations aux dérivées partielles*. Dunod: Paris, 1968 (in French).
23. Gill PE, Murray W, Wright MH. *Practical Optimization*. Academic Press: New York, 1982.
24. Nocedal J, Wright SJ. *Numerical Optimization*. Springer: Berlin, 2002.
25. Lecampion B. Sur l'identification des paramètres des lois de comportement des roches argileuses. *Ph.D. Thesis*, Ecole Polytechnique, 2002.